Designing a Single Protein-Chain Reporter for Opioid Detection at Cellular Resolution

Kayla E. Kroning and Wenjing Wang*

Abstract: *Mu-opioid receptor (MOR) signaling regulates multiple neuronal pathways, including those involved in pain, reward, and respiration. To advance the understanding of MOR's roles in pain modulation, there is a need for high-throughput screening methods of opioids in vitro and high-resolution mapping of opioids in the brain. To fill this need, we designed and characterized a genetically encoded fluorescent reporter, called **S**ingle-chain **P**rotein-based **O**pioid **T**ransmission **I**ndicator **T**ool for MOR (M-SPOTIT). M-SPOTIT represents a new and unique mechanism for fluorescent reporter design and can detect MOR activation, leaving a persistent green fluorescence mark for image analysis. M-SPOTIT showed an opioid-dependent signal to noise ratio (S/N) up to 12.5 and was able to detect as fast as a 30-second opioid exposure in HEK293T cell culture. Additionally, it showed an opioid-dependent S/N up to 4.6 in neuronal culture and detected fentanyl with an EC_{50} of 15 nM. M-SPOTIT will potentially be useful for high-throughput detection of opioids in cell cultures and cellular-resolution detection of opioids in vivo. M-SPOTIT's novel mechanism can be used as a platform to design other G-protein-coupled receptor-based sensors.*

Introduction

Mu-opioid receptor (MOR) signaling regulates multiple neuronal pathways, including those involved in pain, reward, and respiration.[1] Synthetic opioids have been developed to target MOR for effective pain suppression but can also result in addiction, tolerance, and respiratory depression.[1] It is important to study the site-of-action of opioids to understand their functional effects. Therefore, there is a need to detect the general activation of MOR by opioids in a high-throughput manner and to map where opioids act in the brain at cellular resolution.

Existing methods to screen for opioids for MOR in cell cultures are limited by either low throughput, low dynamic range, or specificity for β-arrestin-2 pathway. These methods have taken advantage of two steps in the opioid signaling cascade: the binding of the opioid to the receptor and the downstream signaling events catalyzed by the receptor

activation. Measuring the binding of the opioid to the receptor, through the use of radiolabeled opioids,[2] can be used to infer binding affinities but is low-throughput and does not give information about the efficacy of the ligand in activating MOR. Assays that utilize downstream signaling events to screen for opioids include measuring β-arrestin-2 recruitment, receptor internalization, G-protein recruitment, cyclic AMP (cAMP) levels, and membrane polarization. The former two kinds of assays rely on the receptor's interaction with β-arrestin-2 after receptor activation.[3] Therefore, these two kinds of assays are not optimal for detecting the general activation of the opioid receptor, because there are biased opioid agonists that would preferentially activate the G-protein pathway over the arrestin pathway, resulting in weak arrestin recruitment.[4] G-protein assays involve the incorporation of radiolabeled GTPγS to the activated G-protein but are technically challenging because of radiolabeling and membrane protein extraction.[5] Assays using chimeric $G_{\alpha i}$/ $G_{\alpha q}$ proteins measure the increase of intracellular calcium after opioid activation but require artificial coupling of the chimeric G-proteins with the receptor which is less efficient than endogenous G-protein coupling.[6] cAMP assays, such as those using a transcriptional reporter, have poor dynamic range because opioid receptor-induced cAMP inhibition rarely exceeds 60% of the basal state.[7] Finally, membrane polarization caused by opioid receptor activation can be measured either with recording electrodes[8] or fluorescent membrane potential dyes. Electrical recordings are manually challenging and cannot be used for high-throughput selection. Fluorescent membrane dyes that change intensity due to membrane polarization can be used as an indicator for opioid receptor activation, but these dyes only have approximately a 35–50% decrease of membrane fluorescence.[9]

Current methods for detecting opioids and opioid peptides in the animal brain are limited by spatial resolution. State-of-the-art methods using microdialysis coupled to nano-flow liquid chromatography-mass spectrometry (nLC-MS) enable detection of multiple neuropeptides and other neurotransmitters simultaneously.[10] However, microdialysis nLC-MS methods have poor spatial resolution, limited by the probe size on the order of 500 μm.[10] Fast scan cyclic voltammetry (FSCV) has improved spatial resolution due to its smaller probe size of ≈5 μm in diameter, but FSCV has only been used to detect met-enkephalin and not other opioids.[11]

Due to the limitations of existing methods for detecting opioids for MOR, either low-throughput, small dynamic range, low-spatial resolution, or bias towards the β-arrestin-2 pathway, there is a need for an assay that allows high-throughput detection of the activation of MOR at high spatial

[*] K. E. Kroning, Prof. Dr. W. Wang
Life Sciences Institute, University of Michigan
210 Washtenaw Ave, Ann Arbor, MI 48109 (USA)
and
Department of Chemistry, University of Michigan
930 N University Ave, Ann Arbor, MI 48109 (USA)
E-Mail: wenjwang@umich.edu

resolution. To address this need, we designed a genetically encoded tool, M-SPOTIT, short for **S**ingle-chain **P**rotein-based **O**pioid **T**ransmission **I**ndicator **T**ool for **M**OR. M-SPOTIT represents a new mechanism for fluorescent reporter design. When activated by opioids, M-SPOTIT leaves a persistent fluorescence mark on the cell membrane. We will refer to the ratio between the SPOTIT fluorescence in the presence of opioids to the fluorescence in the absence of opioids as the signal-to-noise ratio, abbreviated as S/N, throughout this paper. We demonstrated that M-SPOTIT can selectively detect agonists for MOR with an opioid-dependent S/N up to 12.5 and can detect a 30-second pulse of opioid exposure in cell cultures.

Results and Discussion

Design and Mechanistic Understanding of SPOTIT

In the general design of SPOTIT, the circularly permuted green fluorescent protein[12] (cpGFP) is inserted between the C-terminus of an opioid receptor and a $G_{\alpha i}$-mimic nanobody, Nb39[13] (Figure 1a). Our initial design rationale was inspired by previous cpGFP-based sensors[12,14,15] where the cpGFP fluorophore is pre-formed and exposed to solvent when cpGFP is in an open conformation. When the sensor is activated, cpGFP changes to a closed conformation, thereby changing the fluorophore's electrostatic environment, which could lead to an immediate fluorescence increase. We, therefore, designed the sensor as shown in Figure 1a so that cpGFP would adopt an open-conformation without opioids and change to a closed-conformation when Nb39 interacts with the activated receptor in the presence of opioids.

We designed M-SPOTIT and the kappa-opioid receptor (KOR) version, K-SPOTIT. FLAG tag was added at the extracellular side for characterizing the sensor expression level. We first checked the opioid response of these two sensors by monitoring their fluorescence immediately after addition of opioid agonists. Initially, we did not observe fluorescence increase; however, 24 hours after opioid agonist incubation, the KOR-sensor showed a S/N of 10.9 in the presence of the synthetic KOR agonist, Salvinorin A (Sal A), compared to the condition without Sal A (Figure 1b). However, the MOR-sensor did not show any fluorescence increase (Supporting Information, Figure S1a). These sensors were named K- and M-SPOTIT1.0. To design a functional M-SPOTIT, we decided to first interrogate the SPOTIT mechanism using K-SPOTIT1.0.

Because the fluorescence of K-SPOTIT1.0 did not increase immediately upon agonist addition as we anticipated, we next probed the working mechanism of the K-SPOTIT1.0 fluorescence increase in response to KOR agonists. We first evaluated the sensor's fluorescence increase at different time points with continuous agonist stimulation and observed that the fluorescence gradually increased over a time course of 24 hours (Figure 1c and Supporting Information, Figure S2). This contradicts our initial sensor design rationale that the fluorescence change would happen instantaneously. Because the change in the electrostatic environment surrounding the cpGFP fluorophore upon opioid-induced conformational change should be fast, it cannot be the cause of the fluorescence increase in K-SPOTIT1.0. Additionally, immunostaining of K-SPOTIT1.0 indicated the sensor expression level is comparable (< 1-fold change) in the presence and absence of Sal A (Figure 1b and Supporting Information, Figure S1b). This suggested the ≈ 10-fold fluorescence increase in the presence of opioid agonists is not due to elevated
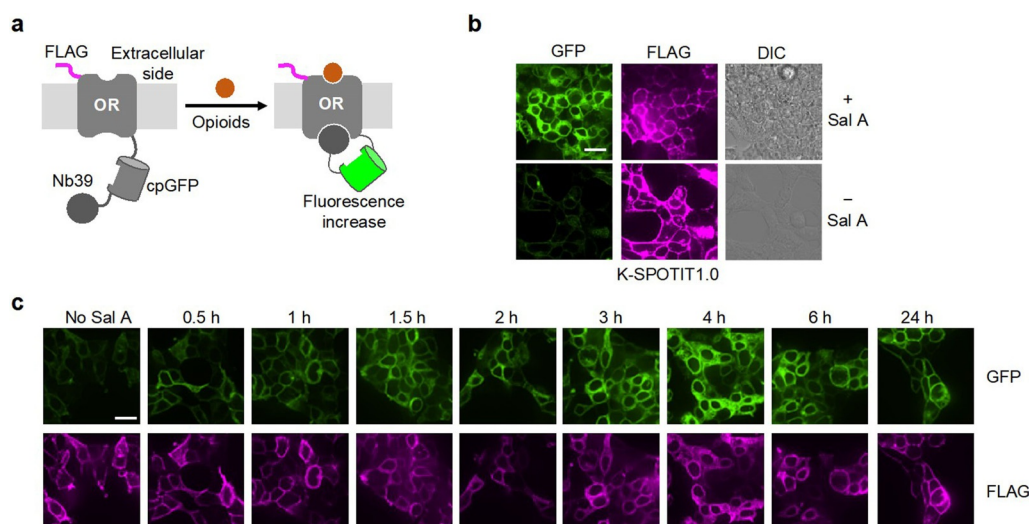

Figure 1. Design and characterization of K-SPOTIT1.0. a) Schematic of SPOTIT. Opioids induce a conformational change in cpGFP, resulting in an increased green fluorescence. OR, opioid receptor; Nb39, $G_{\alpha i}$ protein mimic nanobody 39; cpGFP, circularly permuted GFP from GCaMP6. b) Testing K-SPOTIT1.0 in HEK293T cells. Two days after infection with lentiviruses expressing K-SPOTIT1.0, cells were stimulated with 10 µM Salvinorin A (Sal A) for 24 hours and then fixed and imaged at pH 7. c) K-SPOTIT1.0 fluorophore maturation assay. Two days after infection with lentiviruses expressing K-SPOTIT1.0, cells were stimulated at different time points with 10 µM Sal A for the indicated time periods, and then fixed at the same time point, immunostained, and imaged at pH 7. GFP, cpGFP fluorescence; FLAG, sensor protein expression; h, hour. Scale bars, 20 µm.

protein level or increased protein stability over time. Therefore, we deduced the slow rate of the fluorescence increase in the presence of the agonist is most likely due to fluorophore maturation, which takes approximately 40 minutes for Enhanced Green Fluorescent Protein[16] and maybe even longer for cpGFP. Based on these observations, we hypothesized that the cpGFP's fluorophore in K-SPOTIT1.0 cannot mature in the basal state (without agonists); opioid agonist activation leads to the KOR-Nb39 bound state, allowing the fluorophore to mature.

Next, we examined how the conformational state of the sensor affects the matured sensor's fluorescence. We added KOR antagonist, nor-binaltorphimine (Nor-BNI), to dissociate Nb39 from KOR after 6 hours of agonist incubation, when the K-SPOTIT1.0 fluorophore has already been matured. Comparable fluorescence was observed before and after addition of Nor-BNI (Supporting Information, Figure S3). Therefore, the conformational state after fluorophore maturation does not affect K-SPOTIT1.0's fluorescence.

To further interrogate the necessity of the KOR-Nb39 bound state in the sensor activation, we deleted Nb39 from K-SPOTIT1.0. Surprisingly, Nb39 deletion resulted in high background fluorescence in the absence of agonists (Figure 2 and Supporting Information, Figure S4), indicating the fluorophore of cpGFP was already matured. Additionally, no fluorescence increase was observed after agonist incubation. This led us to further hypothesize that Nb39 is responsible for preventing the cpGFP fluorophore from maturing in the basal

state of K-SPOTIT1.0. Next, we changed Nb39 to Nb80, a $G_{\alpha s}$-mimic nanobody,[17] which does not bind to the activated KOR. High background fluorescence was also observed, indicating that Nb39, uniquely, causes the inability of cpGFP's fluorophore to mature (Figure 2c and d). To further test the generality of Nb39 in inhibiting cpGFP fluorophore maturation, we constructed soluble cpGFP-Nb39 and cpGFP alone (Figure 2e and f). As expected, cpGFP-Nb39 had low fluorescence signal while cpGFP alone had high fluorescence signal (Figure 2e–g). These studies suggest that Nb39 could interact with cpGFP intramolecularly in a unique manner, preventing the fluorophore from maturing; when KOR in K-SPOTIT1.0 is activated, Nb39 interacts with the receptor rather than cpGFP, allowing the fluorophore to mature.

With a better understanding of the SPOTIT mechanism, we next probed the sensor sensitivity to agonist exposure time. We reasoned that the interaction between the activated KOR and Nb39 in SPOTIT will be enhanced due to their close proximity within a single protein chain. Consequently, the agonist-induced KOR-Nb39 bound state could remain stable even after the agonist is removed from the environment. As a result, a short pulse of agonist exposure could also lead to sensor activation as long as the sensor was further incubated to allow fluorophore maturation. To test this, K-SPOTIT1.0 was treated with a short pulse of Sal A and then the agonist was removed. The cells were further incubated for a total of 24 hours (Figure 3a). Figure 3b and c show that a pulse of Sal A stimulation as short as 30 seconds was sufficient to activate K-SPOTIT1.0 with a S/N of 4.2, while longer
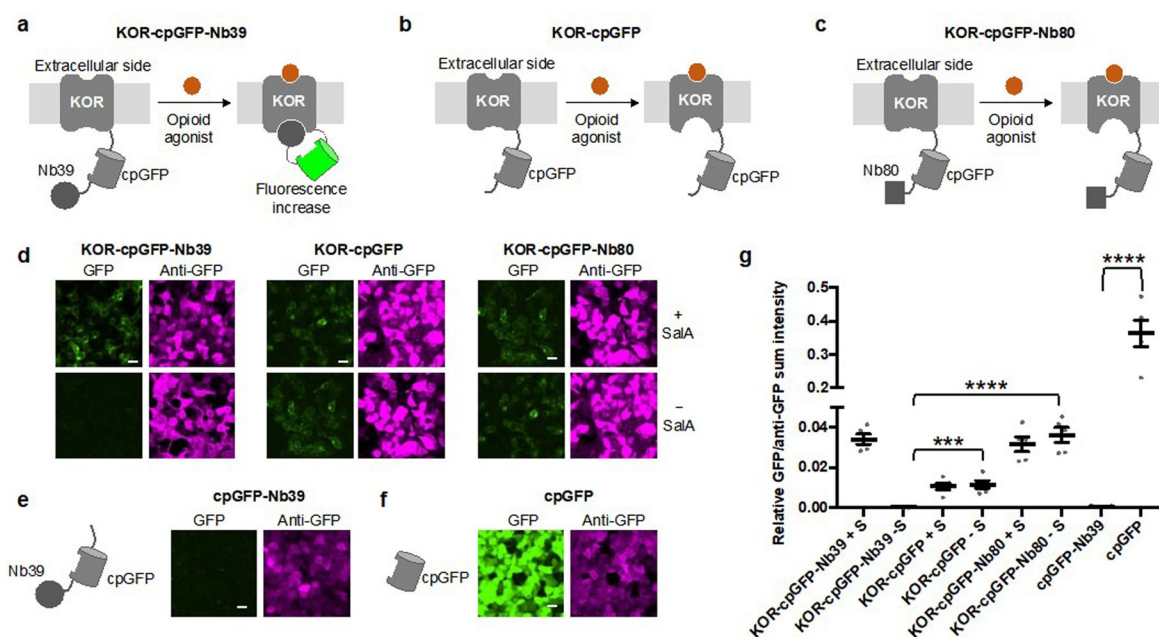

Figure 2. Mechanistic studies of the role of Nb39 in inhibiting K-SPOTIT1.0 fluorophore maturation in the absence of agonists. a–c) Schematics of different constructs for SPOTIT mechanistic studies. d) Confocal imaging of the constructs in (a)–(c) in HEK293T cells. Two days after SPOTIT lentiviral infection, cells were stimulated with 10 µM Sal A for 24 hours and then fixed and immunostained for imaging at pH 7. e,f) Testing Nb39 in inhibiting cpGFP fluorophore maturation. Two days after cpGFP-Nb39 and cpGFP lentiviral infection, cells were fixed and immunostained for imaging at pH 7. g) Analysis of the imaging experiments from (a)–(f). Error bars, standard error of the mean. The mean is represented by the thicker horizontal bar. Stars indicate significance after performing an unpaired Student's t-test. Four stars indicate a p-value < 0.0001. Three stars indicate a p-value of 0.001. $n = 5$ for all conditions. GFP, cpGFP fluorescence; Anti-GFP, protein expression; + S, + Sal A, − S, − Sal A. Scale bars, 20 µm.
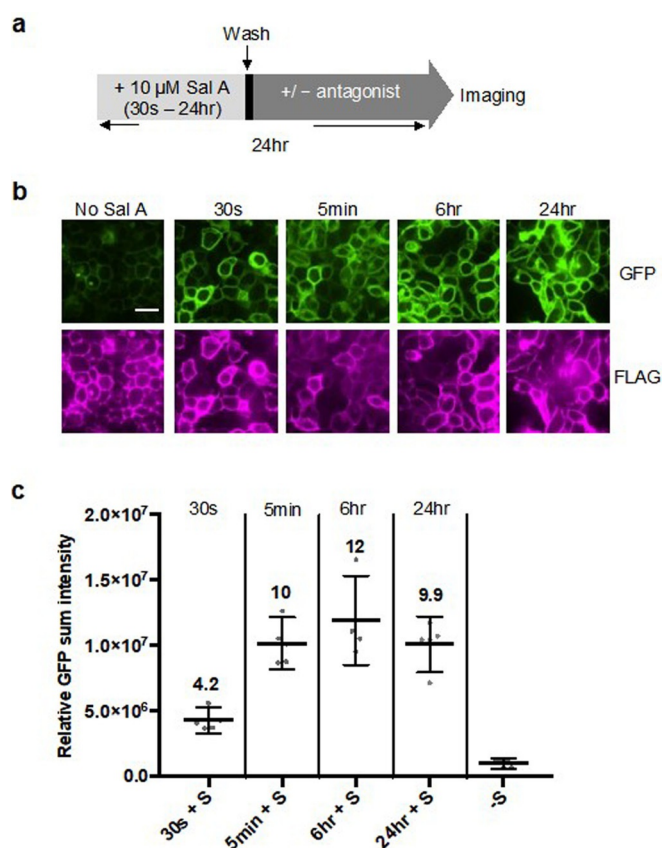
Figure 3. Testing the sensitivity of K-SPOTIT1.0 to agonist exposure time. a) Schematic for characterizing K-SPOTIT1.0 agonist exposure time dependence. Cells were stimulated with 10 µM Sal A for different time periods as indicated in (a), and then Sal A was removed and cells were further incubated for a total of 24 hours. b) Imaging characterization of K-SPOTIT1.0 agonist exposure time dependence in fixed and immunostained HEK293T cells at pH 7. GFP, cpGFP fluorescence; FLAG, sensor protein expression. Scale bar, 20 µm. c) Analysis of agonist exposure time dependence from the imaging experiment in (b). Values above the dots represent the S/N. Error bars, standard error of the mean. The mean is represented by the thicker horizontal bar. $n = 5$ for all conditions. $+ S$, $+ Sal A$; $- S$, $- Sal A$.

incubation lead to a S/N of 12. This suggested that the agonist-induced KOR-Nb39 bound state can be stabilized after a brief opioid exposure; therefore, SPOTIT could be sensitive to short exposure of opioid agonists. To further test the importance of a stable KOR-Nb39 complex for SPOTIT activation, we added KOR antagonist, Nor-BNI, immediately after the initial 30-second agonist stimulation, and the cells were further incubated for 24 hours. We expected antagonist addition to disrupt the KOR-Nb39 bound state of the sensor, preventing the further maturation of the fluorophore. Indeed, no significant fluorescence increase was observed if Nor-BNI was added after the initial opioid exposure in comparison to Nor-BNI-only cells (Supporting Information, Figure S5).

Lastly, to further optimize K-SPOTIT, we varied the linkers connecting the KOR and cpGFP, because previous optimizations of cpGFP-based sensors suggested the linkers connecting the other protein domains and cpGFP are important for sensor performance.[12,15] Additionally, the C-terminal domain of the KOR is important for its interaction

with β-arrestin-2 and subsequent endocytosis after receptor activation. To minimize the sensor interaction with β-arrestin-2, we made different truncations of the intracellular C-terminal domain of the receptor after the palmitoyl cysteine (Supporting Information, Figure S6a). The truncated version, K-SPOTIT1.1, with ten amino acids after the palmityl cysteine, had comparable brightness to K-SPOTIT1.0. The more truncated form, K-SPOTIT1.2, led to a lower signal, illustrating the importance of this linker for SPOTIT's function (Supporting Information, Figure S6b and c). Titration curves were performed with K-SPOTIT1.0, 1.1, and 1.2 to further compare the sensors' performances. All three had similar dynamic ranges, but K-SPOTIT1.1 exhibited the highest sensitivity (Supporting Information, Figure S6d–f).

Design of Functional M-SPOTIT

After dissecting the mechanism of SPOTIT, we focused on designing a functional M-SPOTIT, because MOR is the opioid receptor most involved in pain modulation and addiction.[1] The first design of M-SPOTIT1.0 showed low background fluorescence, presumably because of the same inhibition of the cpGFP fluorophore maturation from Nb39. However, it did not show fluorescence increase upon agonist addition (Supporting Information, Figure S1). This is possibly because the cytosolic domain of MOR is not optimal to allow Nb39 to interact with the agonist-bound MOR. Nb39, therefore, cannot dissociate from cpGFP, and this inhibits cpGFP fluorophore maturation. Because the cytosolic domain of KOR is effective in K-SPOTIT1.1, we designed a chimeric sensor for M-SPOTIT by replacing the cytosolic domain of the MOR with that of K-SPOTIT1.1 (Figure 4a). This chimeric design, which we named M-SPOTIT1.1, yielded a S/N of 3.2 upon incubation with MOR agonists (Figure 4b and c).

Further characterization of M-SPOTIT1.1 by immunostaining showed that when fixed at pH 7.0, M-SPOTIT1.1's fluorescence significantly decreased (Figure 4b and c). Since the fluorophore of M-SPOTIT was already formed, the decrease of the fluorescence could be due to the protonation of the fluorophore, which is less fluorescent than the deprotonated form (Supporting Information, Figure S7). Presumably, formaldehyde cross-linking could cause a higher fluorophore pK_a or change the pH surrounding the fluorophore. To test whether the fluorescence decrease was due to fluorophore protonation, we transfected HEK293T cells with M-SPOTIT1.1 and compared the fluorescence in live cells or fixed cells at pH 7 and 9. Figure 4c shows that the fentanyl-activated M-SPOTIT1.1 was 12.8-fold higher at pH 9 than at pH 7 in fixed cells. We observed a S/N of 3.2 for live cell, 3.8 for fixed at pH 7, and 5.9 for fixed at pH 9 (Figure 4b, c, and Supporting Information, Figure S8). This validated our hypothesis that cpGFP in M-SPOTIT1.1 is in its protonated state at pH 7 in fixed cells.

To determine the pK_a of the fluorophore, we performed a pH titration for M-SPOTIT1.1 in the following three states: the basal state and the beta-endorphin and fentanyl-activated states. Based on the titration curves, we determined the pK_a of
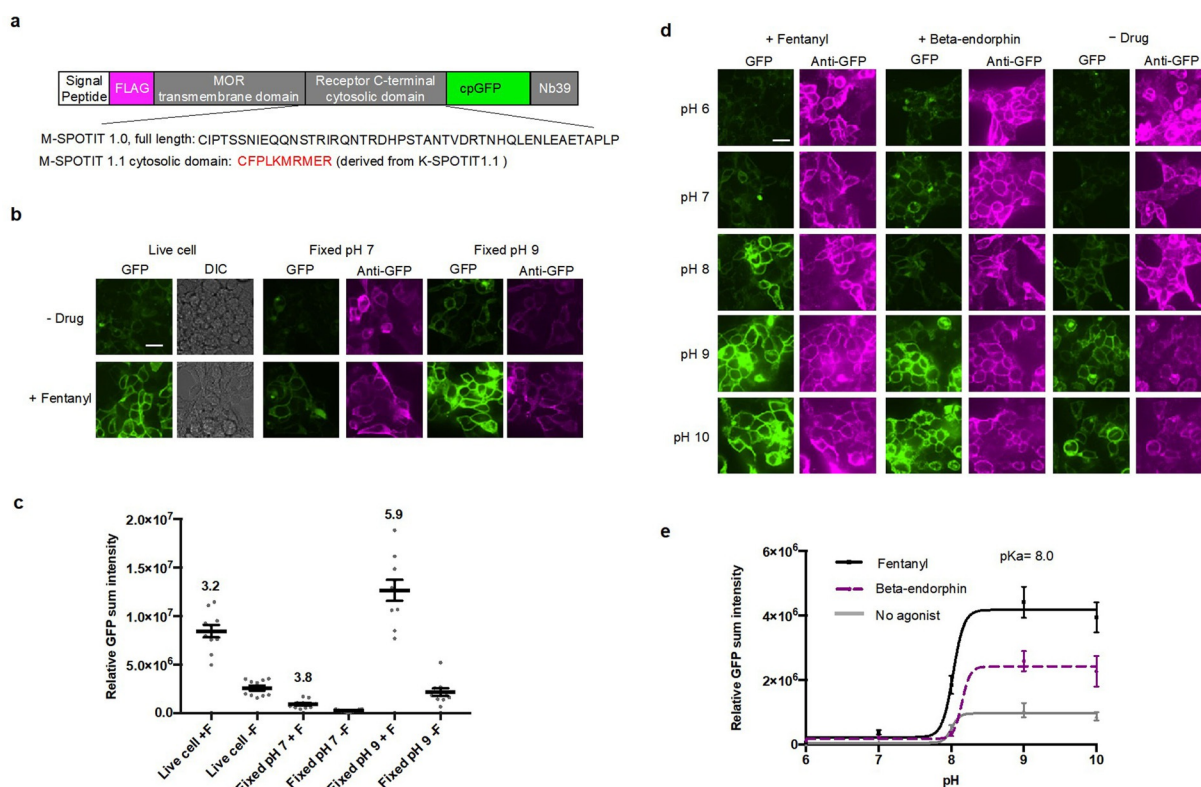
Figure 4. M-SPOTIT1.1 design and pH-dependence. a) DNA constructs of M-SPOTIT1.0 and M-SPOTIT1.1. b) M-SPOTIT1.1 under different imaging conditions. Two days after infection with lentiviruses expressing M-SPOTIT1.1, cells were stimulated with 10 μM fentanyl for 24-hours. Cells were imaged either live or fixed at pH 7 or 9. c) Analysis of the imaging experiment in (b). Error bars, standard error of the mean. The mean is represented by the thicker horizontal bar. Values above the dots represent the S/N. $n = 10$ for each condition. + F, + Fentanyl; − F, − Fentanyl. d) pH titration of M-SPOTIT1.1 in fixed HEK293T cells. Two days after infection with lentiviruses expressing M-SPOTIT1.1, cells were stimulated with 10 μM fentanyl or beta-endorphin for 24 hours and then fixed and immunostained. The cells were then imaged at the pH indicated. e) Analysis of the imaging experiment in (d). Error bars, standard error of the mean. The mean is represented by each point in the plot. $n = 9$–10 for each data point. GFP, cpGFP fluorescence; Anti-GFP, sensor protein expression. Scale bar, 20 μm.

the fluorophore to be 8.0 in fixed cells (Figure 4d, e, and Supporting Information, Figure S9). Therefore, when imaging M-SPOTIT1.1 in formaldehyde-fixed cells, it is important to image at a pH > 8 to observe optimal fluorescence signal. Since the cpGFP fluorophore is fully deprotonated and at its most fluorescent state at pH 10, the different fluorescence observed for M-SPOTIT1.1 with or without agonists indicates different amount of the fluorophore formed. This further supported our hypothesis that the SPOTIT mechanism is based on fluorophore maturation.

Next, we evaluated the sensor maturation time for M-SPOTIT1.1 under continuous opioid stimulation. HEK293T cells expressing M-SPOTIT1.1 were incubated with fentanyl for 30 minutes to 6 hours. Approximately a S/N of 5.8 was observed after 3 hours of fentanyl stimulation, and the fluorescence continued to increase with longer agonist incubation time, resulting in a S/N of 12.5 after 6 hours of fentanyl stimulation (Figure 5a and Supporting Information, Figure S10a). The continuous increase of fluorescence in the presence of fentanyl over time could be due to a combination of gradual fluorophore maturation and continuous activation of the newly translated sensors.

We also tested M-SPOTIT1.1's sensitivity to short pulses of agonist stimulation followed by further incubation without

agonists. M-SPOTIT1.1 was stimulated with a short pulse of agonist exposure, followed by drug removal and further incubation for 24 hours (Figure 5b). Similar to K-SPOTIT, 30 seconds of agonist exposure was sufficient to generate a fluorescence signal for M-SPOTIT1.1 with potent agonists, like fentanyl. Partial agonists, like morphine, required a longer incubation time (Figure 5b and Supporting Information Figure, S10b).

Next, we characterized the selectivity of M-SPOTIT1.1 for MOR agonists. M-SPOTIT1.1 was incubated with various drugs, including MOR peptide agonists, partial and full synthetic MOR agonists, MOR antagonists, and KOR selective agonists. Figure 5c and Supporting Information Figure, S10c show that MOR agonists, such as morphine, fentanyl, buprenorphine, oxycodone, DAMGO, and the peptides leu-enkephalin and beta-endorphin activated M-SPOTIT1.1, illustrating its versatility for a variety of MOR agonists.

Interestingly, DADLE, an agonist for the delta-opioid receptor, could also activate M-SPOTIT1.1, showing a S/N of 2.9. This is consistent with previous studies that suggest DADLE has a weak affinity for MOR.[18] Even more interestingly, isoproterenol activated M-SPOTIT as well, producing a S/N of 2.1. This is also consistent with previous studies that show beta-adrenergic receptor agonists can have
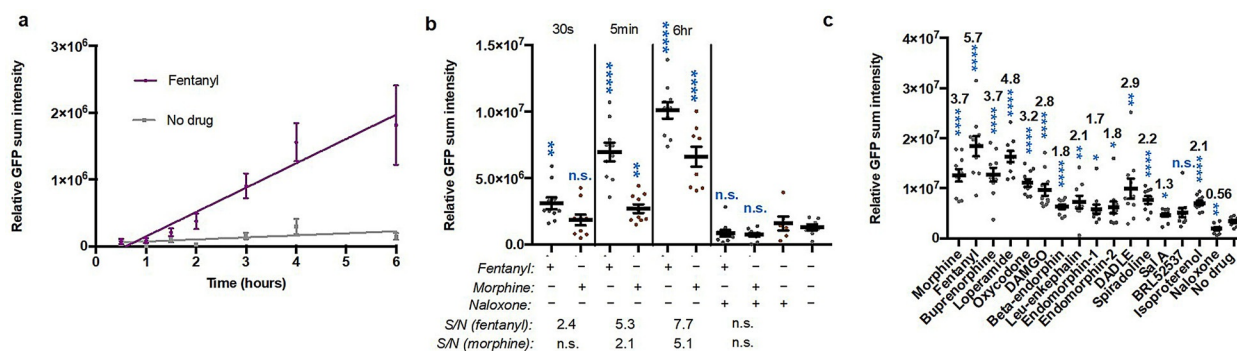
Figure 5. Characterization of M-SPOTIT1.1. a) Characterization of the maturation time dependence of M-SPOTIT1.1. Similar to Figure 1c. 10 μM of fentanyl was used. $n = 9$–10 for each time point. Error bars, standard error of the mean. The mean is represented by each point in the plot. b) Characterization of M-SPOTIT1.1 agonist exposure time dependence. Similar to Figure 3c, M-SPOTIT1.1 was exposed to fentanyl and morphine for different time periods to characterize the sensitivity of the sensor. The MOR antagonist, naloxone, was added after 30 s stimulation to test its inhibition of sensor maturation. 10 μM drug concentration was used for all. Cells were imaged fixed at pH 9 24 hours post-stimulation. S/N was calculated by dividing the sum GFP intensity of the agonist condition and no agonist condition for 30 s, 5 min, and 6 hrs + agonist time points. An unpaired Student's t-test was used to determine the significance between the agonist and no agonist conditions and the agonist + naloxone and only naloxone conditions. Stars indicate significance. Four stars is a p-value < 0.001. Two stars is a p-value of 0.0034 and 0.0036 for 30 s + Fentanyl and 5 min + morphine, respectively. „n.s." indicates no significant difference between compared conditions with p-values of 0.263, 0.1692, and 0.0722 for 30 s + morphine and antagonist conditions, respectively. Error bars, standard error of the mean. The mean is represented by the thicker horizontal bar. $n = 7$–10 for each condition. c) Characterization of M-SPOTIT1.1 drug selectivity. Two days after infection with lentiviruses expressing M-SPOTIT1.1, cells were stimulated with 10 μM of each drug for 24 hours, and then fixed and imaged at pH 9. Error bars, standard error of the mean. The mean is represented by the thicker horizontal bar. Values above the dots represent the S/N. Stars indicate significance after performing an unpaired Student's t-test. Four stars indicate a p-value < 0.0001. Two stars indicate a p-value of 0.0065, 0.0047, and 0.0018 for leu-enkephalin, DADLE, and naloxone, respectively. One star indicates a p-value of 0.0270, 0.0350, and 0.0132 for endomorphin-1, endomorpin-2, and sal A, respectively. „n.s." indicates no significant difference with a p-value of 0.0853. $n = 8$–10 for each condition.

activity towards opioid receptors.[19] This shows that M-SPOTIT1.1's response to different drugs is positively correlated to the drug's ability to activate MOR. It is important to note that we did notice the S/N could vary slightly from experiment to experiment, possibly because the S/N is also affected by other factors including differences in protein expression levels and cell health.

Testing M-SPOTIT1.1 in Cultured Neurons

M-SPOTIT1.1 can potentially be used to determine the site-of-action of endogenous and exogenous opioids in an animal brain. To test the feasibility of this application, we expressed M-SPOTIT1.1 in cultured neurons by AAV viral infection. Stimulation of M-SPOTIT1.1 with fentanyl and beta-endorphin led to a S/N of 4.6 and 2.5, respectively (Figure 6a, b, and Supporting Information, Figure S11). The lower S/N of beta-endorphin could possibly be due to the degradation of the peptide or the inability of the peptide to activate sensors not expressed on the cell membrane.

To compare an agonist's binding affinity to M-SPOTIT versus MOR, we performed a fentanyl titration in cultured neurons. M-SPOTIT1.1 had an apparent EC_{50} of 15 nM for fentanyl, which is comparable to the reported IC_{50} value of fentanyl (8.4 nM) for MOR expressed in HEK293T cells[20] (Figure 6c and Supporting Information, Figure S12). This means fentanyl has a similar binding affinity to M-SPOTIT1.1 as MOR.

To our knowledge, this is the first demonstration of a genetically encoded reporter for detecting opioids in

cultured neurons. This shows that M-SPOTIT1.1 could potentially be useful for detecting opioids in the brain. If signal in animal models becomes an issue due to the thin membranes of neuronal processes, M-SPOTIT1.1 can also be expressed in glial cells under a CAG reporter.[21] Sensor expression and performance in glial cells will more closely resemble that seen in HEK293T cells, enabling the detection of endogenous and exogenous opioids.

Discussion on the Design, Mechanism and Advantageous Characteristics of SPOTIT

To enable the detection of opioids for MOR at high spatial resolution, we designed M-SPOTIT1.1. M-SPOTIT1.1 has many advantageous characteristics. First, M-SPOTIT1.1 has a S/N up to 12.5 and is selective for MOR agonists, allowing a new high-throughput approach to detect opioid agonists in cell cultures. M-SPOTIT1.1's activation is positively correlated to the concentration of the opioid agonists and can detect fentanyl with an EC_{50} of 15 nM in cultured neurons. While the sensitivity of M-SPOTIT1.1 towards synthetic opioids is high, its sensitivity towards beta-endorphin is currently low. To improve the sensitivity of M-SPOTIT1.1 towards endogenous opioid peptides, further engineering of the MOR part of the sensor can be performed. The sensor sensitivity might also be improved by engineering a higher-affinity Nb39 variant that can better stabilize the agonist-bound receptor. Additionally, the S/N of M-SPOTIT1.1 can fluctuate based on cell health; poor cell health results in a higher background signal. The background signal can
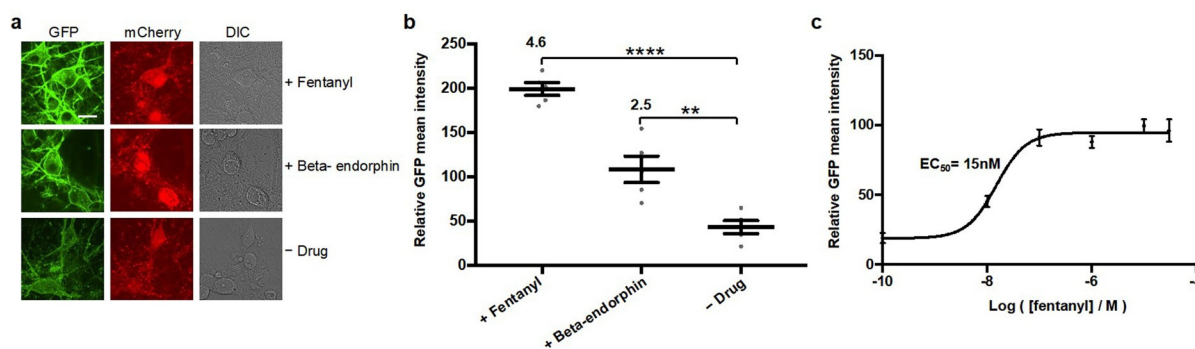
Figure 6. Testing M-SPOTIT1.1 in neuron culture. a) Imaging of M-SPOTIT1.1 in rat cortical neuron culture. Seven days after infection with AAV-viruses expressing TREp-M-SPOTIT1.1-IRES-mCherry and Synapsin-tTA, neurons were stimulated with fentanyl and beta-endorphin for 24 hours. Cells were fixed and imaged at pH 9. GFP, cpGFP fluorescence; mCherry, protein expression level. Scale bar, 20 μm. b) Analysis of the imaging experiment in (a). Error bars, standard error of the mean. The mean is represented by the thicker horizontal bar. Values above the dots represent the S/N. Stars indicate statistical significance analyzed using an unpaired Student's t-test. Four stars indicate a p-value < 0.0001. Two stars indicate a p-value of 0.004. $n = 5$ for each condition. c) Plot of fentanyl titration in cultured neurons. Seven days after infection, M-SPOTIT1.1-infected neurons were stimulated with the indicated concentration of fentanyl. Neurons were fixed and imaged 24-hours post stimulation. Error bars, standard error of the mean. The mean is represented by each point in the plot. $n = 5$ for each condition.

potentially be reduced by enhancing the interaction between Nb39 and cpGFP via directed evolution methods to inhibit cpGFP fluorophore maturation in the basal state.

Second, M-SPOTIT1.1 utilizes a new mechanism to integrate the transient opioid signal to a persistent fluorescent signal, making M-SPOTIT1.1 sensitive to short pulses of opioid stimulation and enabling image analysis at high spatial resolution in fixed cells. Our study shows that the fluorophore maturation of cpGFP in M-SPOTIT1.1 is inhibited by Nb39 in the basal state; opioid agonist-induced intramolecular MOR-Nb39 complex formation allows the cpGFP fluorophore to mature and generate a persistent green fluorescence signal for image analysis. This mechanism was supported by a pH titration of M-SPOTIT1.1, where the sensor was incubated with or without opioids (Figure 4d and e). Both the opioid-incubated and no drug-treated cells showed a pK_a of ≈ 8.0. At pH 9 and 10, the fluorophores are fully deprotonated to their fluorescent state and the green fluorescence signal observed is directly correlated to the amount of cpGFP fluorophore formed. Therefore, the increased green fluorescence observed with opioid incubation over the no opioid condition is due to fluorophore maturation. This mechanism was further supported by the M-SPOTIT maturation assay where longer opioid-incubation time leads to an increased fluorescence when imaged in fixed cells at pH 9. Due to this unique sensor mechanism, M-SPOTIT1.1 can be sensitive to a short-pulse of stimulation when a strong opioid agonist, such as fentanyl, is applied. This is because a stable OR-Nb39 complex can form after a 30-second opioid stimulation and persists, allowing for further fluorophore maturation. SPOTIT will complement the recently developed real-time fluorescent sensors for detecting other GPCR agonists,[14,15] by integrating opioid signals into a persistent fluorescence mark and enabling image analysis across a large brain volume.

SPOTIT represents a new mechanism of reporter design, which can be applied to design other GPCR sensors. For example, this strategy can be used to design sensors for detecting agonists for other $G_{\alpha i}$-coupled GPCRs by fusing the

cpGFP-Nb39 to the C-terminal end of the GPCR. Similar to the M-SPOTIT mechanism, Nb39 will inhibit the cpGFP fluorophore maturation in the basal state. In the presence of agonists, Nb39, as a $G_{\alpha i}$ protein mimic, will interact with the agonist-bound $G_{\alpha i}$-coupled GPCRs, removing the Nb39 from the cpGFP and allowing the cpGFP fluorophore to mature. Some optimization might be needed to improve the binding of Nb39 to other $G_{\alpha i}$-coupled GPCRs in the presence of agonists.

Lastly, M-SPOTIT1.1 is the first single protein chain opioid sensor and only requires one DNA construct for expression, making its performance less protein expression-dependent. Therefore, compared to multiple component reporters such as iTango[22] or split luciferase assay,[23] it will be easier to express M-SPOTIT1.1 in cell cultures and animal models, and M-SPOTIT1.1's performance might be more consistent. M-SPOTIT1.1 could potentially be expressed in neurons for detecting opioids in the brain. It could also be expressed in glial cells under a CAG promoter, enabling higher sensor expression level and hence higher fluorescence signal to determine the localization of opioids in the brain.

Conclusion

Overall, M-SPOTIT1.1 represents the first demonstration of a genetically encoded tool to detect opioid agonists for MOR in HEK293T cells and neurons at cellular resolution. M-SPOTIT1.1 will be useful for screening and characterizing synthetic opioid agonists in cell cultures and can potentially be useful for detecting opioids at cellular resolution in animal models to study the localization of exogenous and endogenous opioids.

Acknowledgements

[1] R. Al-Hasani, M. R. Bruchas, *Anesthesiology* **2011**, *115*, 1363 – 1381.

[2] S. Majumdar, M. Burgman, N. Haselton, S. Grinnell, J. Ocampo, A. R. Pasternak, G. W. Pasternak, *Bioorg. Med. Chem. Lett.* **2011**, *21*, 4001 – 4004.

[3] C. L. Schmid, N. M. Kennedy, N. C. Ross, K. M. Lovell, Z. Yue, J. Morgenweck, M. D. Cameron, T. D. Bannister, L. M. Bohn, *Cell* **2017**, *171*, 1165 – 1175, e13.

[4] T. W. Grim, C. L. Schmid, E. L. Stahl, F. Pantouli, J.-H. Ho, A. Acevedo-Canabal, N. M. Kennedy, M. D. Cameron, T. D. Bannister, L. M. Bohn, *Neuropsychopharmacology* **2020**, *45*, 416 – 425.

[5] R. A. Cerione, *Biochim. Biophys. Acta Rev. Biomembr.* **1991**, *1071*, 473 – 501.

[6] P. Coward, S. D. H. Chan, H. G. Wada, G. M. Humphries, B. R. Conklin, *Anal. Biochem.* **1999**, *270*, 242 – 248.

[7] Y. H. Wong, *Methods Enzymology*, Vol. 238, Academic Press, Cambridge, **1994**, pp. 81 – 94.

[8] V. Spahn, D. Nockemann, H. Machelska in *Methods in Molecular Biology*, Vol. 1230, Humana Press, Clifton, **2015**, pp. 197 – 211.

[9] H. Xing, H.-C. Tran, T. E. Knapp, P. A. Negulescu, B. A. Pollok, *J. Recept. Signal Transduction* **2000**, *20*, 189 – 210.

[10] R. Al-Hasani, J.-M. T. Wong, O. S. Mabrouk, J. G. McCall, G. P. Schmitz, K. A. Porter-Stransky, B. J. Aragona, R. T. Kennedy, M. R. Bruchas, *eLife* **2018**, *7*, e36520.

[11] A. C. Schmidt, L. E. Dunaway, J. G. Roberts, G. S. McCarty, L. A. Sombers, *Anal. Chem.* **2014**, *86*, 7806 – 7812.

[12] T. Nagai, A. Sawano, E. S. Park, A. Miyawaki, *Proc. Natl. Acad. Sci. USA* **2001**, *98*, 3197 – 3202.

[13] W. Huang, A. Manglik, A. J. Venkatakrishnan, T. Laeremans, E. N. Feinberg, A. L. Sanborn, H. E. Kato, K. E. Livingston, T. S. Thorsen, R. C. Kling, S. Granier, P. Gmeiner, S. M. Husbands, J. R. Traynor, W. I. Weis, J. Steyaert, R. O. Dror, B. K. Kobilka, *Nature* **2015**, *524*, 315 – 321.

[14] J. Feng, C. Zhang, J. E. Lischinsky, M. Jing, J. Zhou, H. Wang, Y. Zhang, A. Dong, Z. Wu, H. Wu, W. Chen, P. Zhang, J. Zou, S. A. Hires, J. J. Zhu, G. Cui, D. Lin, J. Du, Y. Li, *Neuron* **2019**, *102*, 745 – 761, e8.

[15] T. Patriarchi, J. R. Cho, K. Merten, M. W. Howe, A. Marley, W.-H. Xiong, R. W. Folk, G. J. Broussard, R. Liang, M. J. Jang, H. Zhong, D. Dombeck, M. von Zastrow, A. Nimmerjahn, V. Gradinaru, J. T. Williams, L. Tian, *Science* **2018**, *360*, eaat4422.

[16] R. Iizuka, M. Yamagishi-Shirasaki, T. Funatsu, *Anal. Biochem.* **2011**, *414*, 173 – 178.

[17] S. G. F. Rasmussen, H.-J. Choi, J. J. Fung, E. Pardon, P. Casarosa, P. S. Chae, B. T. DeVree, D. M. Rosenbaum, F. S. Thian, T. S. Kobilka, A. Schnapp, I. Konetzki, R. K. Sunahara, S. H. Gell-man, A. Pautsch, J. Steyaert, W. I. Weis, B. K. Kobilka, *Nature* **2011**, *469*, 175 – 180.

[18] H. Suh, L. Tseng, *Naunyn-Schmiedeberg's Arch. Pharmacol.* **1990**, *342*, 67 – 71.

[19] R. Root-Bernstein, M. Turke, U. Subhramanyam, B. Churchill, J. Labahn, *Int. J. Mol. Sci.* **2018**, *19*, 272.

[20] P. Gharagozlou, H. Demirci, J. D. Clark, J. Lameh, *BMC Pharmacol.* **2003**, *3*, 1.

[21] P. A. Lawlor, R. J. Bland, A. Mouravlev, D. Young, M. J. During, *Mol. Ther.* **2009**, *17*, 1692 – 1702.

[22] D. Lee, M. Creed, K. Jung, T. Stefanelli, D. J. Wendler, W. C. Oh, N. L. Mignocchi, C. Lüscher, H.-B. Kwon, *Nat. Methods* **2017**, *14*, 495 – 503.

[23] Y. Fujikawa, N. Kato, *Plant J.* **2007**, *52*, 185 – 195.